Chemically induced supramolecular reorganization of triblock copolymer assemblies: Trapping of intermediate states via a shell-crosslinking methodology

Qinggao Ma*, Edward E. Remsen*, Christopher G. Clark, Jr.*, Tomasz Kowalewski†, and Karen L. Wooley*‡

*Department of Chemistry, Washington University, One Brookings Drive, St. Louis, MO 63130; and †Department of Chemistry, Carnegie Mellon University, 4400 Fifth Avenue, Pittsburgh, PA 15213

Edited by Jack Halpern, University of Chicago, Chicago, IL, and approved January 3, 2002 (received for review December 6, 2001)

The mechanism of morphological phase transitions was studied for rod-shaped supramolecular assemblies comprised of a poly(acrylic acid)-*block*-poly(methyl acrylate)-*block*-polystyrene (PAA_{90}-*b*-PMA_{80}-*b*-PS_{100}) triblock copolymer in 33% tetrahydrofuran/water after perturbation by reaction with a positively charged water-soluble carbodiimide. Tetrahydrofuran solvation of the hydrophobic core domain provided the dynamic nature required for the rod-to-sphere phase transition to be complete within 30 min. The intermediate morphologies such as fragmenting rods and pearl-necklace structures were trapped kinetically by the subsequent addition of a diamino crosslinking agent, which underwent covalent crosslinking of the shell layer. Alternatively, shell-crosslinked rod-shaped nanostructures with preserved morphology were obtained by the addition of the crosslinking agent before the addition of the carbodiimide, which allowed for the shell crosslinking to be performed at a faster rate than the morphological reorganization. The formation of robust shell-crosslinked nanostructures provides a methodology by which the morphological evolution processes can be observed, and it allows access to otherwise thermodynamically unstable nanostructures.

The versatility of the solution-state assembly of block copolymers (1, 2) has attracted much interest toward the preparation of unique nanostructured materials possessing different compositions, shapes, and structures (3–12). Controlled assembly of block copolymers depends on a number of factors. The equilibrium between micellar assemblies and individual polymer chains involves a delicate balance of supramolecular polymer–polymer and polymer–solvent interactions, which provides a lever of enthalpic and entropic control (13) for the directed evolution of micellar morphologies with changes in the solution conditions. Studies to determine the kinetics of block copolymer micellization (14–16) and the kinetics and mechanisms for transformation of assembly morphologies (17–19) have become active areas of research. For a given block copolymer composition, the introduction of ions and alteration of the solution pH (20–22), modification of the solvent composition (23–25), and changes in the polymer concentration (26, 27) have been found to effect reorganization of block copolymer supramolecular assemblies. The identification of methodologies that allow for observation (28) and accurate manipulation (19) of the supramolecular assembly processes is critical for the preparation and development of advanced nanostructured materials.

Spherical, rod-like, and vesicular assemblies are observed commonly for the supramolecular assembly of amphiphilic block copolymers. The covalent stabilization of such assemblies is facilitated by regioselective crosslinking chemistry (29, 30), performed within the core domain, throughout the shell layer, or at an intermediate radial layer. It is interesting to note that as focus has shifted from fullerenes to carbon nanotubes for carbon-based nanostructures, interest also has shifted from spherical nanoparticles to cylindrical or rod-like supramolecular assemblies and their intramicellarly crosslinked products (8, 9, 31). Transformations from rods to spheres induced by irradiation with light (32) and alteration of the solvent composition (19, 33) have been studied by a number of techniques in solution and in the solid state. Burke and Eisenberg (19) reported sphere-to-rod and rod-to-sphere transitions for $polystyrene_{310}$-*block*-$poly(acrylic\ acid)_{52}$ diblock copolymer assemblies in a mixture of dioxane and water. The transitions, induced by jumps in solvent composition, each occur via a two-stage process. For the sphere-to-rod transitions, the process required sphere collisions followed by reorganization into smooth cylindrical rods, whereas the rod-to-sphere transitions proceeded by bulb formation at one or both ends of the rod-shaped micelles followed by release of the bulbs in the form of spherical micelles. The rod-to-sphere transformation was described further as occurring exclusively with bulb formation from the end of the rod, with the release of the spherical micelles progressing along the length of the rod until a final sphere is formed ultimately. Trapping of the intermediate assemblies was facilitated by lyophilization, and visualization was by transmission electron microscopy (TEM).

Given the influence that the block copolymer composition plays in the size, shape, and stability of the supramolecular assemblies, triblock copolymers have arisen as a rich material from which to study aggregates containing multilayer morphologies (34–37). In our previous studies of shell-crosslinked nanostructures derived from $poly(acrylic\ acid)_{90}$-*block*-$poly(methyl\ acrylate)_{80}$-*block*-$polystyrene_{100}$ (PAA_{90}-*b*-PMA_{80}-*b*-PS_{100}) self-assembled in a solution of tetrahydrofuran (THF) and water and dialyzed into pure water followed by crosslinking through amidation chemistry within the shell layer, a mixture of spheres and rods was observed (36). In this report we describe investigations designed to probe the supramolecular assembly process and the reorganization of the micellar structures that occurs with changes in their chemical composition *in situ*. In particular, we find that in aqueous solution containing 33 vol% THF, rod-like micelles form initially, which in contrast to the diblock copolymer assemblies (19) transform to spheres by a process that involves at least three discrete steps and more likely involves a continuum of morphological intermediates.

Results and Discussion

Intramicellar crosslinking reactions offer a methodology by which to trap intermediate supramolecular assemblies kinetically

This paper was submitted directly (Track II) to the PNAS office.

Abbreviations: TEM, transmission electron microscopy; THF, tetrahydrofuran; ETC, 1-[3-(dimethylamino)propyl]-3-ethylcarbodiimide methiodide; PAA, poly(acrylic acid); PMA, poly(methyl acrylate); PS, polystyrene; AFM, atomic force microscopy.

‡To whom reprint requests should be addressed at: Department of Chemistry, Washington University, One Brookings Drive, CB 1134, St. Louis, MO 63130-4899. E-mail: klwooley@artsci.wustl.edu.

www.pnas.org/cgi/doi/10.1073/pnas.052653099

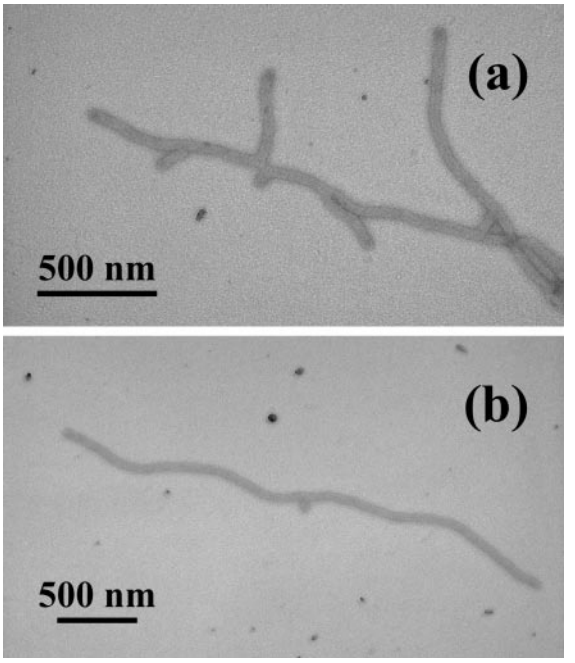

Fig. 1. TEM images (with platinum shadowing) of rod-shaped supramolecular assemblies of PAA_{90}-*b*-PMA_{80}-*b*-PS_{100} formed in THF/water (vol/vol = 1:2, 0.32 mg/ml) and nebulized onto a carbon-coated copper grid.

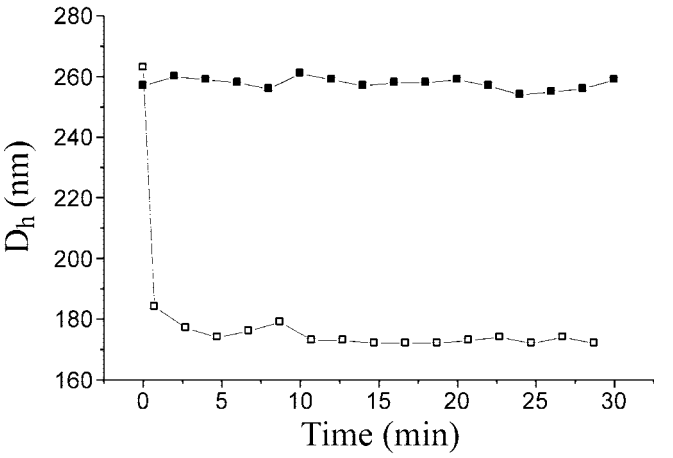

Fig. 2. *In situ* monitoring of the average hydrodynamic diameter values, D_h, as measured by dynamic light scattering for the triblock copolymer assemblies (0.32 mg/ml in 1:2 THF/water, 10 ml) with the introduction of ETC (10 mg in 50 μl water, □) and water (50 μl, ■). The time interval is 2 min.

and thereby allow the real-time monitoring of thermodynamic equilibration processes. In this paper we report the study of rod-shaped micelles from an amphiphilic ABC triblock copolymer, PAA_{90}-*b*-PMA_{80}-*b*-PS_{100} (36), which is transformed into spheres with perturbation by reaction with the water-soluble carbodiimide, 1-[3-(dimethylamino)propyl]-3-ethylcarbodiimide methiodide (ETC). Subsequent intramicellar crosslinking by reaction with the diamine, 2,2′-(ethylenedioxy)bis(ethylamine), is conducted at periodic times as a strategy to preserve the intermediate morphologies for characterization. The establishment of covalent bonds between the polymer chains comprising supramolecular assemblies has been shown to generate robust nanomaterials (38–40) that are not subject to further reorganization events during the evaluation experiments. Therefore, this approach allows for the study of the phase-transition processes under a number of experimental conditions: in solution and in the solid state.

The triblock copolymer PAA_{90}-*b*-PMA_{80}-*b*-PS_{100} self-assembled to form supramolecular structures having a rod-like morphology in a 33 vol% THF/H_2O mixed-solvent system. The rod diameter was 55 ± 2 nm, and the length varied from 160 nm to several microns as observed by TEM (Fig. 1). The hydrophobic core region of the rods was solvated by the THF, as was observed by solution-state ^{1}H NMR data (see the ^{1}H NMR spectra contained within Fig. 7, which is published as supporting information on the PNAS web site, www.pnas.org). At THF concentrations in excess of 30 vol%, protons within the PS chain segments were observed, and resonances for the protons of the PMA chain segments were observed at >15 vol% THF. The solvation of the core region provided for morphological mobility and flexibility.

Rapid transformation of the rod-like assemblies occurred after the introduction of ETC (41, 42). The morphological transformation process was observed *in situ* by dynamic light scattering (Fig. 2). Dynamic light scattering showed that the initial rod-like assemblies had a broad distribution with an average intensity-weighted hydrodynamic diameter value, D_h, of 270 nm. After the addition of ETC, the D_h value dropped quickly to 170 nm, which corresponds to an ≈4-fold decrease in hydrodynamic volume. Control experiments involving the addition of water demonstrated that the decreased D_h was the result of the presence of the ETC and not simply a dilution effect (Fig. 2).

The intermediate morphologies were trapped during the transformation by subsequent addition of the diamino crosslinker 2,2′-(ethylenedioxy)bis(ethylamine) to form covalent amide linkages among the block copolymer acrylic acid chain segments constituting the water-soluble shell layer. Imaging of the samples by atomic force microscopy (AFM) and TEM revealed a rod-to-sphere fragmentation process (Fig. 3) that could be trapped and evaluated at various stages by controlling the timing of the addition of diamine crosslinker. When 2,2′-(ethylenedioxy)bis(ethylamine) was added within 5 min of the ETC addition, intermediate stages of the rod fragmentation were observed by tapping-mode AFM in air (Fig. 3 *a* and *b*), under solution (Fig. 3 *c* and *d*), and by TEM (Fig. 3 *e* and *f*). Each of these images reveals a complex fragmentation mechanism for the rod-to-sphere morphology change in which the rods transform to spheres by "budding" randomly along the rods. As illustrated in Scheme 1[§], the formation of spherically divided rod segments appears to begin first by a constriction around the rod, which becomes more prominent. Loss of spheres can occur from the rod chain end or along the chain and ultimately pearl-necklace structures can result. It is uncertain whether the spheres of the pearl necklace are crosslinked interspherically in addition to being crosslinked intraspherically. The average diameter of the uniform rods was 30 ± 1 nm (measured by TEM). Once the fragmentation process began, the constriction rings at which the spheres developed from the rods gave measured diameters that varied from 10 to 28 nm depending on the degree of fragmentation. The spheres that spawned from the rods were larger in diameter (39 ± 6 nm, measured by TEM) and taller (17 ± 2 vs. 14 ± 2 nm, measured by AFM) than were the rods. The addition of 2,2′-(ethylenedioxy)bis(ethylamine) at longer time intervals (30 and 90 min) after the introduction of ETC gave only spherical shell-crosslinked micelles, as observed by TEM (diameter = 32 ± 3 nm) and AFM (height = 17 ± 2 nm) imaging (Fig. 4). Because a ^{1}H NMR study showed that ETC has a half-life of 41 h

[§]Victor Luaña's TESSEL2 (www.uniovi.es/~quimica.fisica/qcg/tessel/tessel.html), John VanSickle's REORIENT matrix macro (enphilistor.users4.50megs.com/macs.htm), and POV-RAY (www.povray.org/) were used in the generation and rendition of the three-dimensional tesselations. Inference of specific length-scale differences between assemblies caused by changes in morphology should not be drawn from the illustrations.

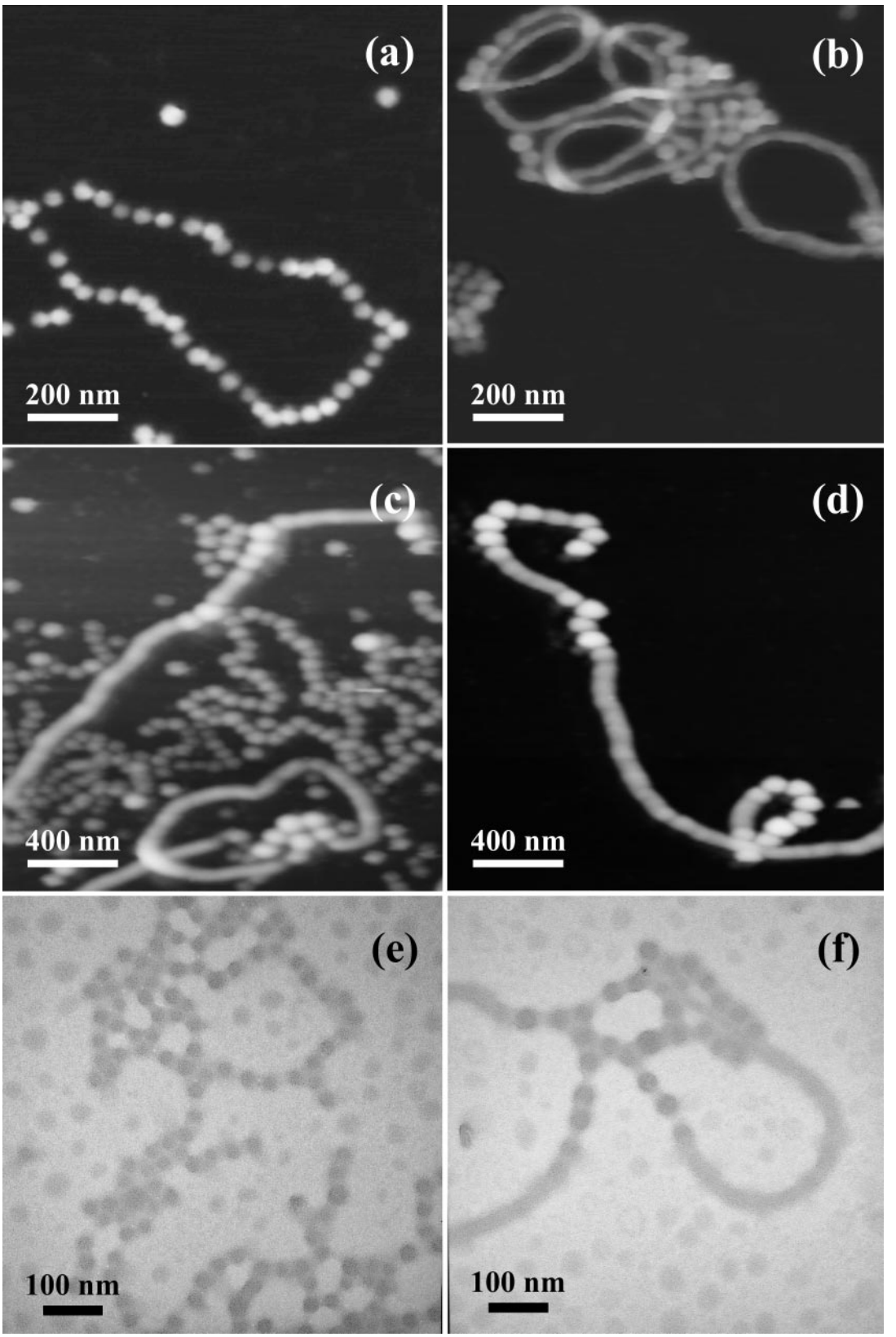

Fig. 3. Imaging of the shell-crosslinked intermediates reveals the rod-to-sphere fragmentation mechanism. The diamino crosslinker, 2,2′-(ethylenedioxy)bis(ethylamine), was added less than 5 min after the addition of ETC to the micelles of PAA_{90}-*b*-PMA_{80}-*b*-PS_{100} in THF/water (vol/vol = 1:2). *a* and *b* were imaged by tapping-mode AFM with sample preparation including drop-deposition onto freshly cleaved mica and drying in air, *c* and *d* were imaged by fluid-tapping AFM under solution on mica in the presence of 10 mM $MgCl_2$, and *e* and *f* were imaged by TEM on a carbon-coated copper grid with platinum shadowing.

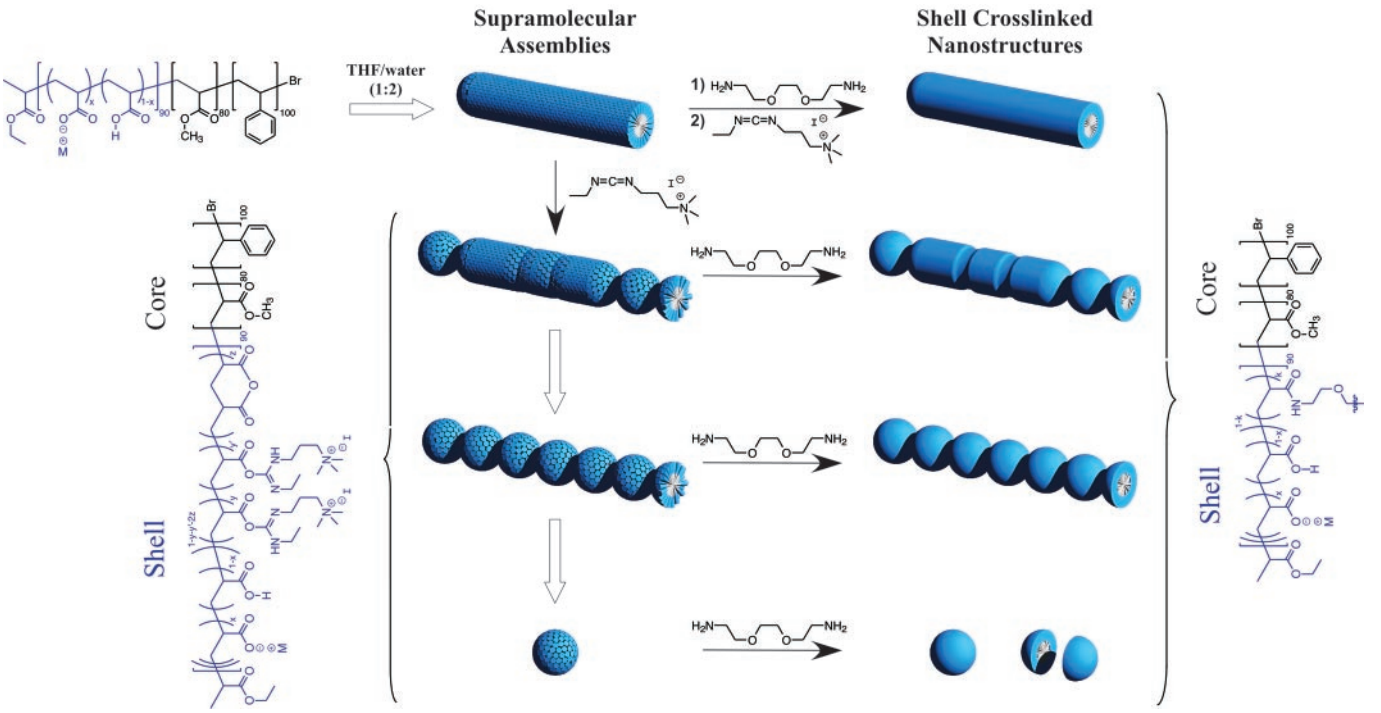

Scheme 1. Illustration of the self assembly of PAA_{90}-*b*-PMA_{80}-*b*-PS_{100} triblock copolymers into cylindrical supramolecular assemblies, followed by kinetic trapping via covalent shell crosslinking to preserve the morphologies at varying degrees of morphological perturbation.

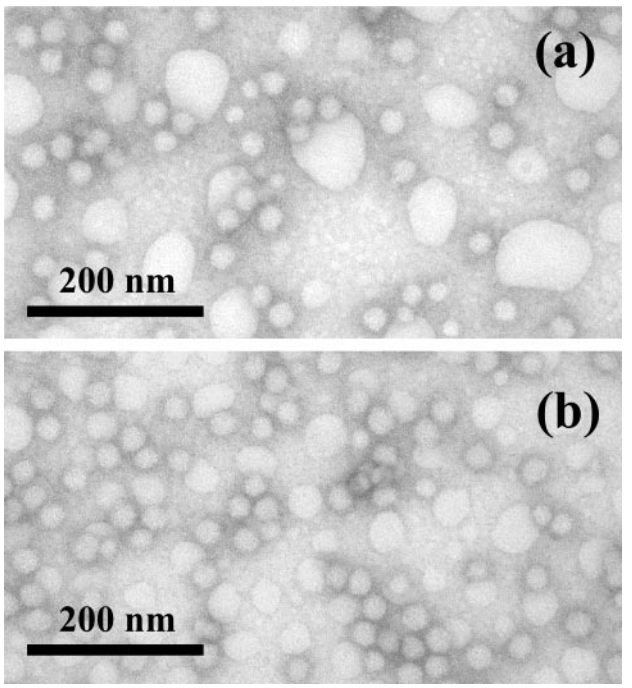

Fig. 4. TEM images (obtained on a carbon-coated copper grid with negative staining by a mixture of uranyl acetate and bacitracin) of shell-crosslinked spherical nanostructures formed by the addition of 2,2′-(ethylenedioxy)bis-(ethylamine) 30 (*a*) and 90 (*b*) min after the addition of ETC to the supramolecular assemblies of PAA_{90}-*b*-PMA_{80}-*b*-PS_{100} in 1:2 THF/water. The large, noncircular bright spots are artifacts of the sample preparation for these TEM images, which included mixing the aqueous solution of the nanostructures with a 2 wt% uranyl acetate containing 20 μg/ml bacitracin (1:1 volume), depositing an 8-μl drop onto a carbon-coated 300-mesh copper grid, allowing the sample to stand for 1 min, wicking off the excess liquid, and allowing the sample to air dry.

in D_2O (see Fig. 8, which is published as supporting information on the PNAS web site), the rod fragmentation entirely to spheres was the result of the PAA chemical modification by reaction with ETC and the subsequent morphological change and was not merely caused by the presence of ETC or its hydrolysis by-products.

With the addition of ETC, reaction with the acrylic acid functionalities present in the shell layer of the rod-shaped supramolecular assemblies produced *O*-acylisourea (43–45) and anhydride (see Fig. 9, which is published as supporting information on the PNAS web site) active intermediates. Therefore, the composition of the triblock copolymer comprising the rod-

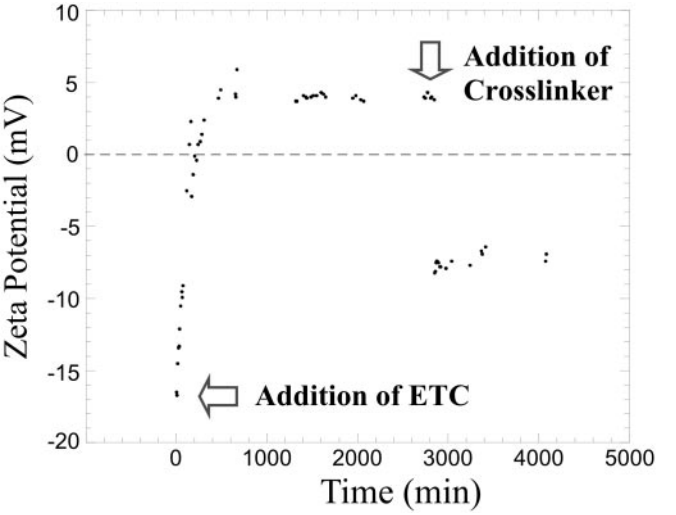

Fig. 5. ζ-potential data for the PAA_{90}-*b*-PMA_{80}-*b*-PS_{100} triblock assemblies [0.32 mg/ml, 10 ml in THF/water, 1:2 (vol/vol)] after the addition of ETC (20 mg) and subsequent addition of 2,2′-(ethylenedioxy)bis(ethylamine) (2 mg).

like micelles was altered, which resulted in evolution of the amphiphilic core-shell rod morphology. It is unclear whether the rod-to-sphere morphological transition is caused by alteration in the local coulombic interactions within the nanostructures, a change in solvation or hydrophilicity of the shell layer, or a combination of these factors. The formation of *O*-acylisourea intermediates was supported by ξ-potential measurements (Fig. 5) obtained by electrophoretic light scattering. The values of ξ changed from negative (-18 mV) to positive (4 mV) over time after the addition of ETC and conversion of carboxylic acids and/or carboxylates to *O*-acylisoureas bearing the quaternary ammonium group. Because ξ is a measure of the electric field potential at the object's plane of zero shear, it is affected by the size, shape, and surface charge of the structure. The ξ value reflects the change in chemical composition and morphology and reached a plateau at $\approx$400 min. After the addition of the diamine crosslinker, the ξ again returned to a negative value (-8 mV), indicating that not all carboxylates were consumed by the crosslinking chemistry (46).

To preserve the rod-like morphology for PAA_{90}-*b*-PMA_{80}-*b*-PS_{100} in the mixed THF/water solution, the crosslinking reaction must occur faster than does the morphology transformation. Experimentally, this preservation was accomplished by introduction of the diamino crosslinker before the addition of ETC. The presence of the diamino crosslinker did not change the morphology of the micelle, as was observed by dynamic light scattering. The surfaces of the resulting shell-crosslinked rod-shaped nanostructures formed by this approach were smooth with diameters of 30 $\pm$ 1 nm (TEM) and height values of 15 $\pm$ 2 nm (AFM); no budding of spheres could be observed along the rod (Fig. 6).

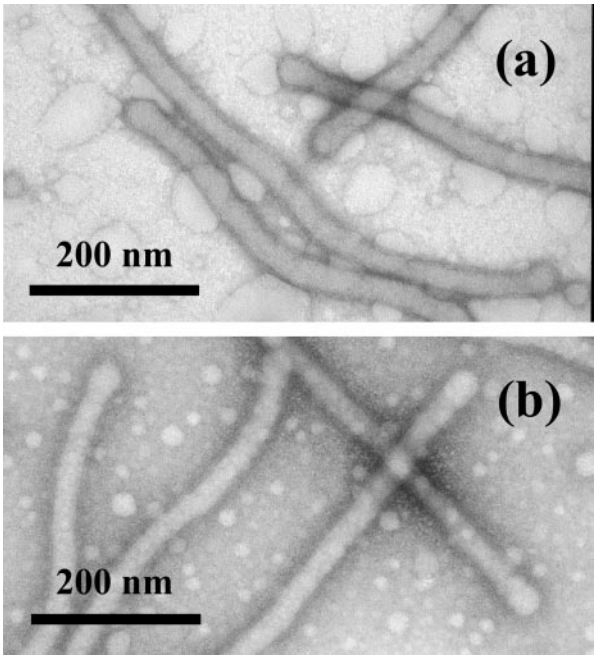

Fig. 6. TEM images (obtained on a carbon-coated copper grid with negative staining by a mixture of uranyl acetate and bacitracin) of shell-crosslinked rod-shaped nanostructures formed by the addition of ETC 30 (*a*) and 90 (*b*) min after the addition of 2,2′-(ethylenedioxy)bis(ethylamine) to the supramolecular assemblies of PAA_{90}-*b*-PMA_{80}-*b*-PS_{100} in 1:2 THF/water. The large, noncircular bright spots are artifacts of the sample preparation for these TEM images, which included mixing the aqueous solution of the nanostructures with a 2 wt% uranyl acetate containing 20 μg/ml bacitracin (1:1 volume), depositing an 8-μl drop onto a carbon-coated 300-mesh copper grid, allowing the sample to stand for 1 min, wicking off the excess liquid, and allowing the sample to air dry.

Conclusions

In summary, crosslinking reactions facilitated the kinetic trapping of the supramolecular assemblies formed from triblock copolymers in water. Addition of a small molecule reagent perturbed the assembly, and the intermediate nanostructures resulting from supramolecular reorganization were isolated and identified. Additional studies are required to understand the effects of the addition of perturbation agents to supramolecular polymer assemblies. The strategy involving the intentional perturbation of supramolecular assemblies and trapping at intermediate stages may serve as a general methodology for investigation of other systems. Moreover, this methodology allows for access to novel nanostructured materials including those that are not available as thermodynamically stable morphologies (in analogy to the comparison of kinetic vs. thermodynamic products in small molecule syntheses).

We thank Mr. G. Michael Veith for TEM measurements. We also extend appreciation to the Malvern Company for providing the Zetasizer on which the ζ-potential measurements were conducted. Funding of this research by the National Science Foundation (DMR-9974457) and the Army Research Office (DAAG55-98-1-0046) is gratefully acknowledged.

1. Zhang, L. & Eisenberg, A. (1995) *Science* **268,** 1728–1731.
2. Zhang, L. & Eisenberg, A. (1996) *J. Am. Chem. Soc.* **118,** 3168–3181.
3. Stupp, S. I., Son, S., Lin, H. C. & Li, L. S. (1993) *Science* **259,** 59–63.
4. Thurmond, K. B., II, Kowalewski, T. & Wooley, K. L. (1996) *J. Am. Chem. Soc.* **118,** 7239–7240.
5. Guo, A., Liu, G. & Tao, J. (1996) *Macromolecules* **29,** 2487–2493.
6. Bütün, V., Lowe, A. B., Billingham, N. C. & Armes, S. P. (1999) *J. Am. Chem. Soc.* **121,** 4288–4289.
7. Discher, B. M., Won, Y.-Y. Ege, D. S., Lee, J. C.-M., Bates, F. S., Discher, D. E. & Hammer, D. A. (1999) *Science* **284,** 1143–1146.
8. Won, Y., Davis, H. T. & Bates, F. S. (1999) *Science* **283,** 960–963.
9. Stupp, S. I. & Osenar, P. (1999) *Mater. Sci. Technol.* **20,** 513–547.
10. Stewart, S. & Liu, G. (2000) *Angew. Chem. Int. Ed. Eng.* **39,** 340–344.
11. Sanji, T., Nakatsuka, Y., Ohnishi, S. & Sakurai, H. (2000) *Macromolecules* **33,** 8524–8526.
12. Cao, L., Manners, I. & Winnik, M. A. (2001) *Macromolecules* **34,** 3353–3360.
13. Whitesides, G. M., Simanek, E. E., Mathias, J. P., Seto, C. T., Chin, D. N., Mammen, M. & Gordon, D. M. (1995) *Acc. Chem. Res.* **28,** 37–44.
14. Bednár, B., Edwards, K., Almgren, M., Tormod, S. & Tuzar, Z. (1988) *Makromol. Chem.* **9,** 785–790.
15. Honda, C., Hasegawa, Y., Hirunuma, R. & Nose, T. (1994) *Macromolecules* **26,** 7660–7668.
16. Hecht, E. & Hoffmann, H. (1995) *Colloids Surf. A* **96,** 181–197.
17. Iyama, K. & Nose, T. (1998) *Macromolecules* **31,** 7356–7364.
18. Chen, L., Shen, H. & Eisenberg, A. (1999) *J. Phys. Chem. B* **103,** 9488–9497.
19. Burke, S. & Eisenberg, A. (2001) *Langmuir* **21,** 6705–6714.
20. Zhang, L., Yu, K. & Eisenberg, A. (1996) *Science* **272,** 1777–1779.
21. Martin, T. J., Prochazka, K., Munk, P. & Webber, S. E. (1996) *Macromolecules* **29,** 6071–6073.
22. Shen, H., Zhang, L. & Eisenberg, A. (1999) *J. Am. Chem. Soc.* **121,** 2728–2740.
23. Yu, Y., Zhang, L. & Eisenberg, A. (1998) *Macromolecules* **31,** 1144–1154.
24. Yu, Y. & Eisenberg, A. (1997) *J. Am. Chem. Soc.* **119,** 8383–8384.
25. Stamouli, A., Pelletier, E., Koutsos, V., van der Vegte, E. & Hadziioannou, G. (1996) *Langmuir* **12,** 3221–3224.
26. Liang, Y., Li, Z. & Li, F. (2000) *Chem. Lett.* 320–321.
27. Zhang, L. & Eisenberg, A. (1999) *Macromolecules* **32,** 2239–2249.
28. Massey, J., Power, K. N., Manners, I. & Winnik, M. A. (1998) *J. Am. Chem. Soc.* **120,** 9533–9540.
29. Clark, C. G., Jr. & Wooley, K. L. (2002) in *Dendrimers and Other Dendritic Polymers*, eds. Fréchet, J. M. J. & Tomalia, D. A. (Wiley, New York).
30. Becker, M. L., Remsen, E. E. & Wooley, K. L. (2001) *J. Polym. Sci.* [*A1*] **39,** 4152–4166.
31. Yu, G. & Eisenberg, A. (1998) *Macromolecules* **31,** 5546–5549.
32. Brückner, E., Sonntag, P. & Rehage, H. (2001) *Langmuir* **17,** 2308–2311.
33. Lin, T.-L., Chen, S.-H., Gabriel, N. E. & Roberts, M. F. (1990) *J. Phys. Chem.* **94,** 855–862.

34. Patrickios, C. S., Forder, C., Armes, S. P. & Billingham, N. C. (1997) *J. Polym. Sci.* [*A1*] **35,** 1181–1195.
35. Kriz, J., Massar, B., Plestil, J., Tuzar, Z., Posipisil, H. & Doskociloca, D. (1998) *Macromolecules* **31,** 41–51.
36. Ma, Q. & Wooley, K. L. (2000) *J. Polym. Sci.* [*A1*] **38,** 4805–4820.
37. Underhill, R. S. & Liu, G. (2000) *Chem. Mater.* **12,** 2082–2091.
38. Remsen, E. E., Thurmond, K. B., II & Wooley, K. L. (1999) *Macromolecules* **32,** 3685–3689.
39. Huang, H., Remsen, E. E., Kowalewski, T. & Wooley, K. L. (1999) *J. Am. Chem. Soc.* **121,** 3805–3806.
40. Won, Y.-Y., Paso, K., Davis, H. T. & Bates, F. S. (2001) *J. Phys. Chem. B* **105,** 8302–8311.
41. Wooley, K. L. (2000) *J. Polym. Sci.* [*A1*] **38,** 1397–1407.
42. Zhang, Q., Remsen, E. E. & Wooley, K. L. (2000) *J. Am. Chem. Soc.* **122,** 3642–3651.
43. Ibrahim, I. T. & Williams, A. (1980) *Chem. Commun.* 25–27.
44. Rebek, J. & Feitler, D. (1973) *J. Am. Chem. Soc.* **95,** 4052–4053.
45. Williams, A. & Ibrahim, I. T. (1981) *J. Am. Chem. Soc.* **103,** 7090–7095.
46. Huang, H., Wooley, K. L. & Schaefer, J. (2001) *Macromolecules* **34,** 547–551.